

Zirconia phase effect in Pd/ZrO₂ catalyzed CO₂ hydrogenation into
formate

Zhenhua Zhang^{†*}, Liyuan Zhang[‡], Max J. Hülsey[†], Ning Yan^{†,*}

[†]Department of Chemical and Biomolecular Engineering, National University of Singapore,
Blk E5, 4 Engineering Drive 4, Singapore 117585

[‡]Hefei National Laboratory for Physical Sciences at Microscale, CAS Key Laboratory of
Materials for Energy Conversion and Department of Chemical Physics, University of Science
and Technology of China, Hefei 230026, P. R. China

*To whom correspondence should be addressed. E-mail: hanyuzh@mail.ustc.edu.cn;
ning.yan@nus.edu.sg

Chemicals and materials

Monoclinic and tetragonal zirconia were supplied by Saint-Gobain NorPro. Other chemicals were purchased from Sigma-Aldrich. All chemicals are used without further purification.

Characterizations

The Pd loadings in the catalysts were determined using an iCAP 6000 series inductively coupled plasma optical emission spectrometer (ICP-OES). The catalysts were digested in nitric acid (68 wt %) at 80 °C overnight and then diluted with deionized water to a desired volume before analysis. Powder X-ray diffraction (XRD) patterns were acquired on a Philips X’Pert PROS diffractometer using a nickel-filtered Cu K α (wavelength: 0.15418 nm) radiation source with the operation voltage being 40 kV and operation current being 50 mA. The powder catalysts were firstly pressed into a small tablet, then held on the sample holder, and finally tested. X-ray photoelectron spectroscopy (XPS) spectra were acquired on an ESCALAB 250 high performance electron spectrometer using monochromatized Al K α ($h\nu=1486.7$ eV) as the excitation source. The samples were stuck on the stage and tested. The binding energy of samples was calibrated by setting the adventitious carbon (C1s) to 284.8 eV. Transmission electron microscopy (TEM) and high-resolution transmission electron microscopy (HRTEM) measurements were analysed on a JEM 2100F (JEOL, Japan) high resolution transmission electron microscope. The operation voltage was 200 kV. The samples were dispersed in ethanol. One drop of the ethanol dispersion was then placed on an extra-thick copper grid. The acquired copper grid was fixed on the sample stage for analysis.

H₂-temperature programmed reduction (H₂-TPR) and CO₂-temperature programmed desorption (CO₂-TPD). H₂-TPR and CO₂-TPD experiments were performed on a Micromeritics Autochem 2920 apparatus equipped with a TCD detector. In the H₂-TPR experiment, 20 mg as-synthesized fresh catalyst without reduction was put into a quartz reactor and heated at 5 K min⁻¹ in 5% H₂ balanced with Ar with a flow rate of 30 mL min⁻¹.

The result was recorded by the TCD detector. In the CO₂-TPD experiment, 100 mg as-synthesized fresh catalyst without reduction was firstly reduced by 5% H₂ balanced with N₂ with a flow rate of 30 mL min⁻¹ at 473 K for 1 h, then switched to pure Ar with a flow rate of 30 mL min⁻¹ and heated to 673 K for another 1 h, next cooled down to room temperature in Ar atmosphere. The acquired catalyst was immersed into pure CO₂ with a flow rate of 50 mL min⁻¹ for 2 h and purged by Ar with a flow rate of 30 mL min⁻¹ at room temperature. Finally, the acquired catalyst was heated at 5 K min⁻¹ in pure Ar with a flow rate of 30 mL min⁻¹ and the results were recorded by the TCD detector.

In situ diffuse reflectance infrared Fourier transformed spectra (DRIFTS). *In situ* DRIFTS experiments were performed on a Nicolet iS50 FT-IR spectrometer equipped with a high temperature DRIFTS reaction cell (Harrick Scientific Products, INC) using an MCT/A detector in the series mode with 64 scans and at a resolution of 4 cm⁻¹. The detailed procedures for *in situ* DRIFTS of CO adsorption, CO₂ + H₂ experiments, and CO₂, H₂ sequential treatments experiments are provided in the supporting information.

For *in situ* DRIFTS of CO adsorption experiments, 50 mg as-synthesized sample without reduction was loaded on the sample stage and heated in 5% H₂ balanced with N₂ with a flow rate of 30 mL min⁻¹ to 473 K at a rate of 5 K min⁻¹ and kept for 1 h afterwards. Then the atmosphere was switched to pure N₂ with a flow rate of 30 mL min⁻¹ at 473 K for another 30 min, before cooling down to room temperature in N₂ atmosphere. The spectra were recorded in N₂ atmosphere at room temperature as the background. Then 5% CO balance with N₂ with a flow rate of 50 mL min⁻¹ was admitted for 1 h, and finally purged with pure N₂ with a flow rate of 30 mL min⁻¹. The DRIFTS spectra were recorded during the N₂ purge. For *in situ* DRIFTS of CO₂ + H₂ experiments, the catalyst was firstly reduced by 5% H₂/N₂ at 473 K, following the same procedure as described for the *in situ* DRIFTS of CO adsorption. After collecting background spectra under N₂ flow, the DRIFTS spectra were recorded in CO₂ + H₂

atmosphere with the ratio of 1:1 for 30 min. For *in situ* DRIFTS of sequential exposure to CO₂ and H₂ experiments, the catalyst was firstly reduced by 5% H₂/N₂ at 473 K, then treated with N₂ flow to collect the background, and finally purge with pure H₂ or CO₂ with a flow rate of 25 mL min⁻¹. The DRIFTS spectra were recorded in the presence of H₂ or CO₂ flow at 373 K for 30 min. Next CO₂ + H₂ (1:1) at a flow rate of 50 mL/min was admitted into the cell at 373 K for 30 min, during which the DRIFTS spectra were also recorded.

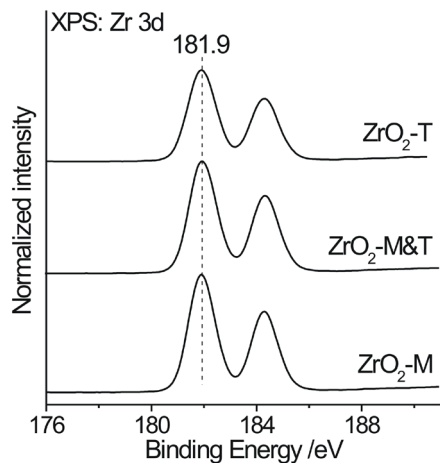


Figure S1. Zr 3d XPS spectra of various ZrO_2 catalysts.

Table S1. Pd loading (weight %) of various Pd/ ZrO_2 catalysts determined by OES-ICP; The specific BET surface areas of various ZrO_2 ; The number of CO_2 desorption of various ZrO_2 and 2%Pd/ ZrO_2 catalysts.

Catalysts	Pd loadings (wt. %)	BET surface area (m^2/g)	Pore volume (cm^3/g)	Pore diameter (nm)	Number of CO_2 desorption ($\mu\text{mol/g}$)
$\text{ZrO}_2\text{-M}$	-	103	0.3	10.8	154.6
0.01%Pd/ $\text{ZrO}_2\text{-M}$	0.0095	-			-
0.1%Pd/ $\text{ZrO}_2\text{-M}$	0.097	-			-
2%Pd/ $\text{ZrO}_2\text{-M}$	1.907	-			229.1
$\text{ZrO}_2\text{-M&T}$	-	85	0.23	10.2	348.7
0.01%Pd/ $\text{ZrO}_2\text{-M&T}$	0.0094	-			-
0.1%Pd/ $\text{ZrO}_2\text{-M&T}$	0.091	-			-
2%Pd/ $\text{ZrO}_2\text{-M&T}$	1.921	-			172.4
$\text{ZrO}_2\text{-T}$	-	123	0.29	10.9	637.9
0.01%Pd/ $\text{ZrO}_2\text{-T}$	0.0093	-			-
0.1%Pd/ $\text{ZrO}_2\text{-T}$	0.092	-			-

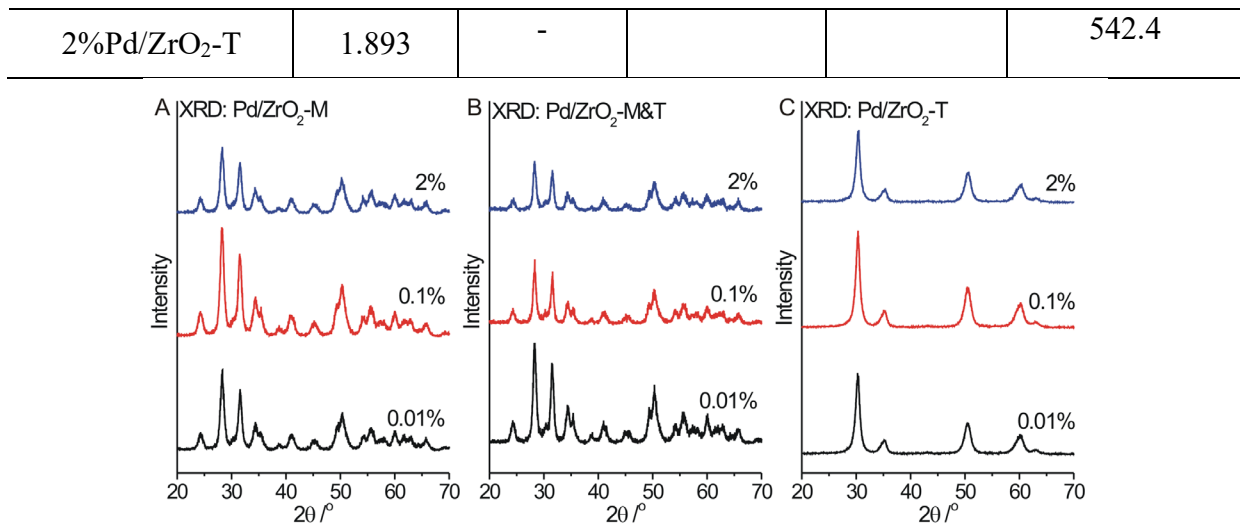


Figure S2. XRD patterns of various (A) Pd/ZrO₂-M, (B) Pd/ZrO₂-M&T, and (C) Pd/ZrO₂-T catalysts.

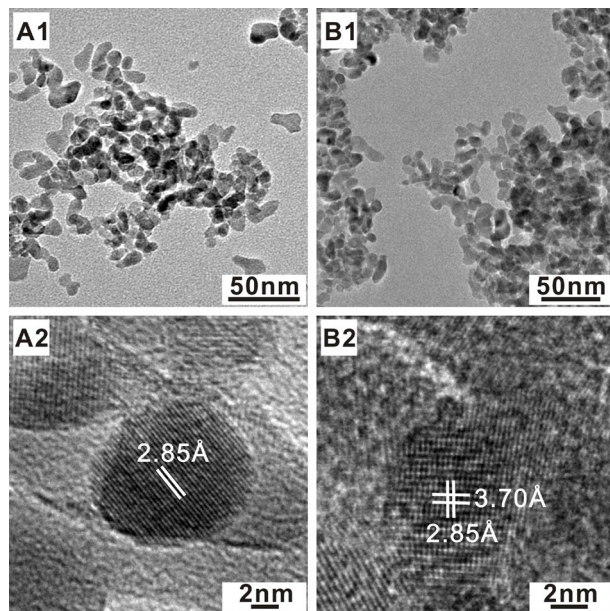


Figure S3. TEM and HRTEM images of (A1, A2) 0.01%Pd/ZrO₂-M and (B1, B2) 0.1%Pd/ZrO₂-M catalysts. The lattice fringes of 2.85 and 3.70, respectively, correspond to the spacing of monoclinic ZrO₂{111} and monoclinic ZrO₂{110} (JCPDS card NO. 37-1484) crystal planes.

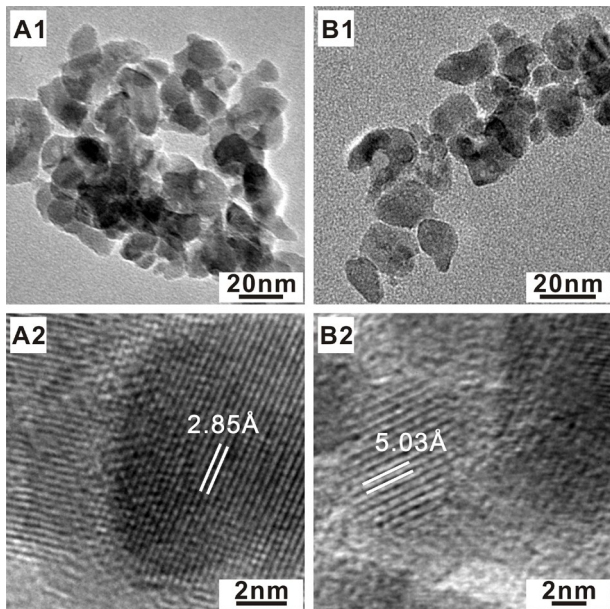


Figure S4. TEM and HRTEM images of (A1, A2) 0.01%Pd/ZrO₂-M&T and (B1, B2) 0.1%Pd/ZrO₂-M&T catalysts. The lattice fringes of 2.85 and 5.03 Å, respectively, correspond to the spacing of monoclinic ZrO₂{111} (JCPDS card NO. 37-1484) and monoclinic ZrO₂{001} crystal planes.

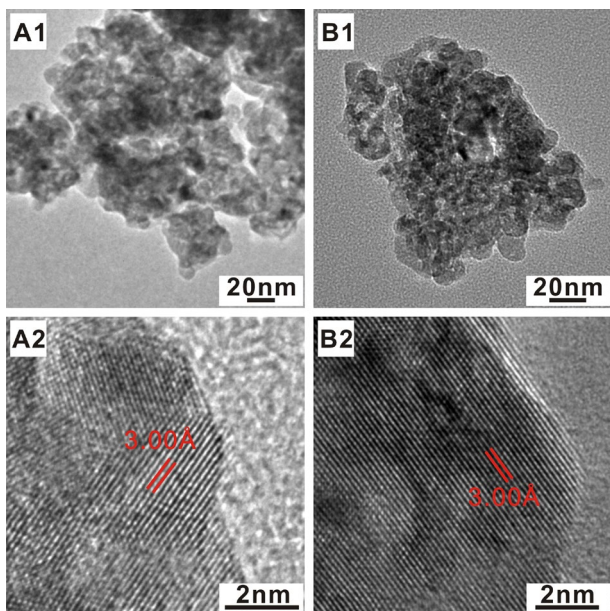


Figure S5. TEM and HRTEM images of (A1, A2) 0.01%Pd/ZrO₂-T and (B1, B2) 0.1%Pd/ZrO₂-T catalysts. The lattice fringes of 3.00 Å correspond to the spacing of tetragonal ZrO₂{101} (JCPDS card NO. 42-1164) crystal plane.

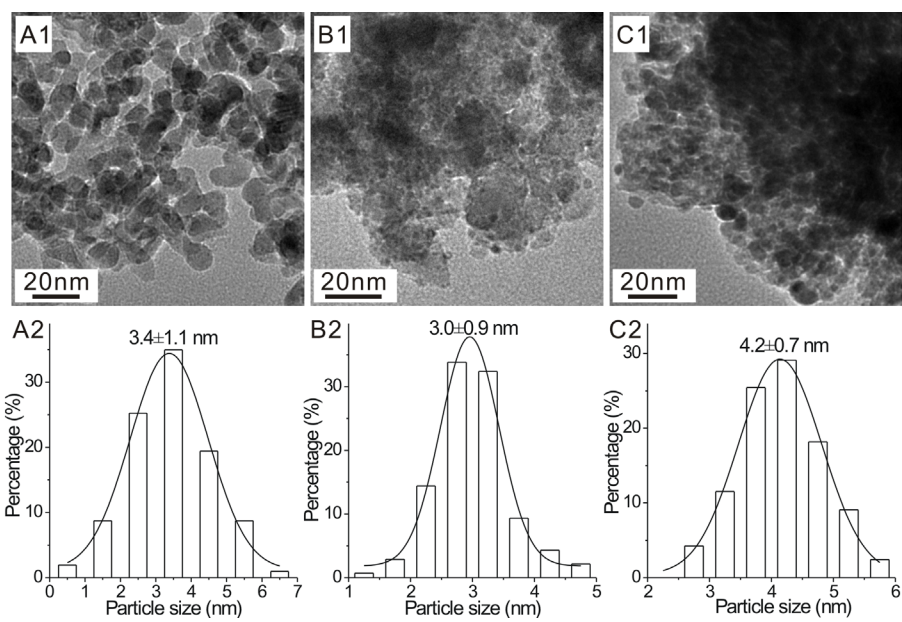


Figure S6. TEM images and the size distributions of (A1, A2) 2%Pd/ZrO₂-M, (B1, B2) 2%Pd/ZrO₂-M&T, and (C1, C2) 2%Pd/ZrO₂-T catalysts.

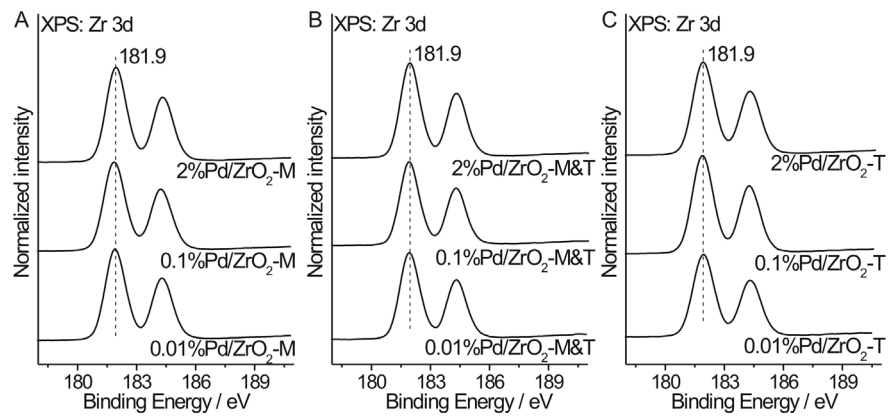


Figure S7. Zr3d XPS spectra of (A) various Pd/ZrO₂-M, (B) various Pd/ZrO₂-M&T, and (C) various Pd/ZrO₂-T catalysts.

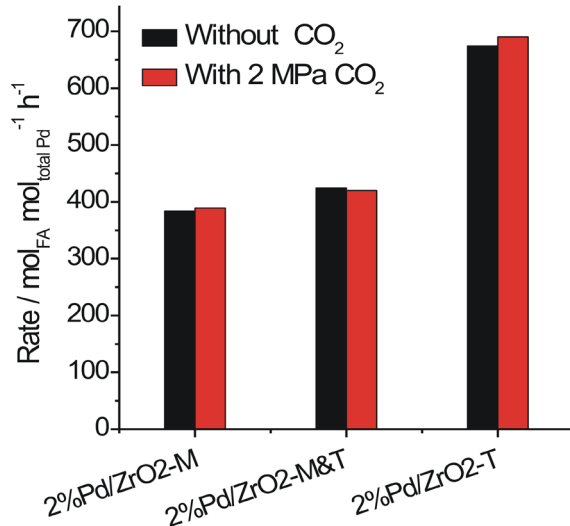


Figure S8. Production rate ($\text{mol}_{\text{FA}} \text{ mol}_{\text{total Pd}}^{-1} \text{ h}^{-1}$) of FA on representative various 2%Pd/ZrO₂ catalysts at the reaction conditions (2 MPa H₂, 373 K, and 168 mg NaHCO₃) with and without CO₂.

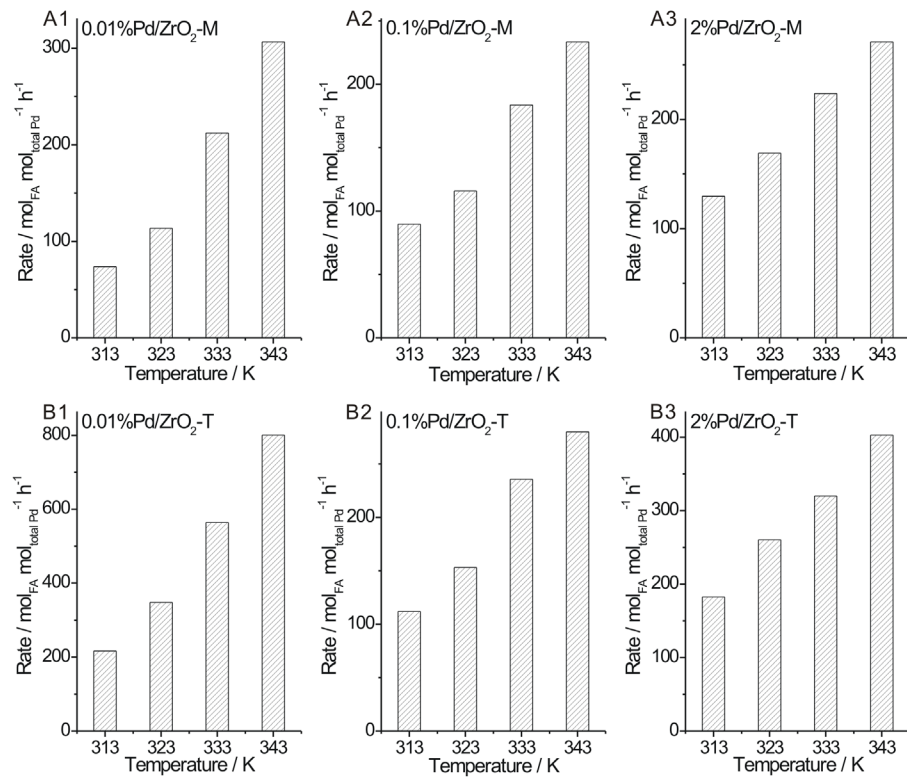


Figure S9. (A) Production rate ($\text{mol}_{\text{FA}} \text{ mol}_{\text{total Pd}}^{-1} \text{ h}^{-1}$) of FA at different reaction temperature on (A1-A3) various Pd/ZrO₂-M and (B1-B3) various Pd/ZrO₂-T catalysts based on the total Pd atoms.

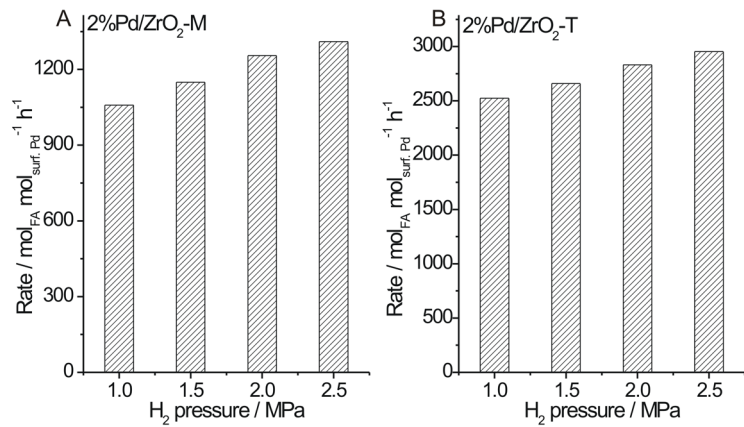


Figure S10. (A) Production rate (mol_{FA} mol_{surf. Pd}⁻¹ h⁻¹) of FA at the condition of 168 mg NaHCO₃ and various pressures of H₂ (MPa) on (A) 2%Pd/ZrO₂-M and (B) 2%Pd/ZrO₂-T catalysts based on the surface Pd atoms.

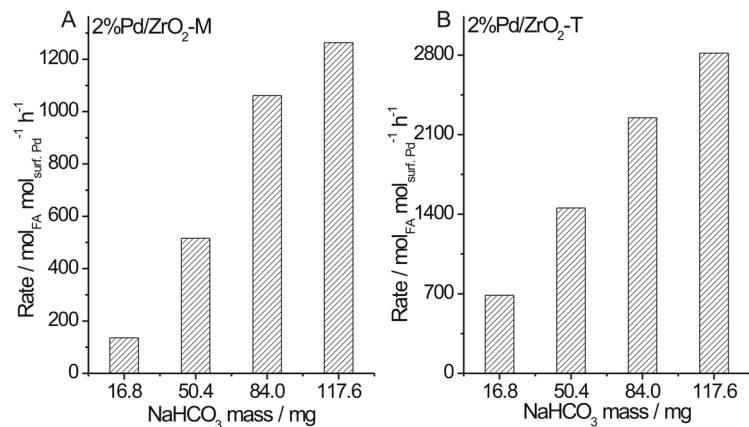


Figure S11. (A) Production rate (mol_{FA} mol_{surf. Pd}⁻¹ h⁻¹) of FA at the condition of 2 MPa H₂ and various masses of NaHCO₃ (mg) on (A) 2%Pd/ZrO₂-M and (B) 2%Pd/ZrO₂-T catalysts based on the surface Pd atoms.

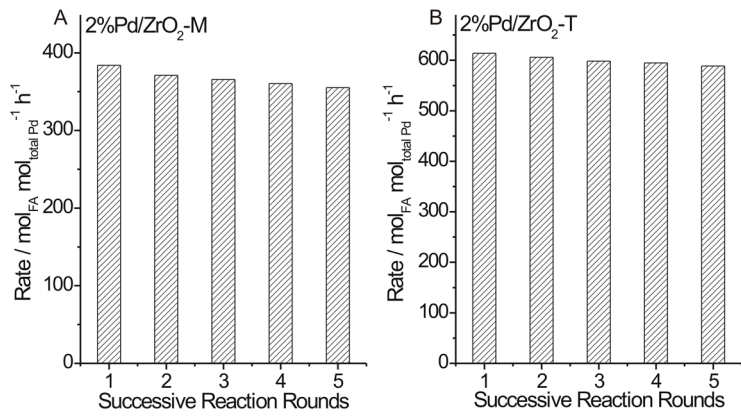


Figure S12. Production rate ($\text{mol}_{\text{FA}} \text{ mol}_{\text{total Pd}}^{-1} \text{ h}^{-1}$) of FA on (A) 2%Pd/ZrO₂-M and (B) 2%Pd/ZrO₂-T catalysts over five successive rounds at 373 K.

Table S2. Assignment of vibrational bands in the DRIFTS spectra of surface species at various Pd/ZrO₂ catalysts.

Assignment	Schematic structure	Bands (cm ⁻¹)	Ref.
Bicarbonate		1470~1487 1613~1630	[1-4]
Bidentate carbonate		1304~1316 1510~1541 1684~1691	[3,4]
Bidentate formate		1375~1380 1595~1599	[5,6]
Monodentate carbonate		1354~1358 1439~1459	[4]
CO adsorption on Pd(0)	-	1841~1848 1900~1908 2018~2037	[7]

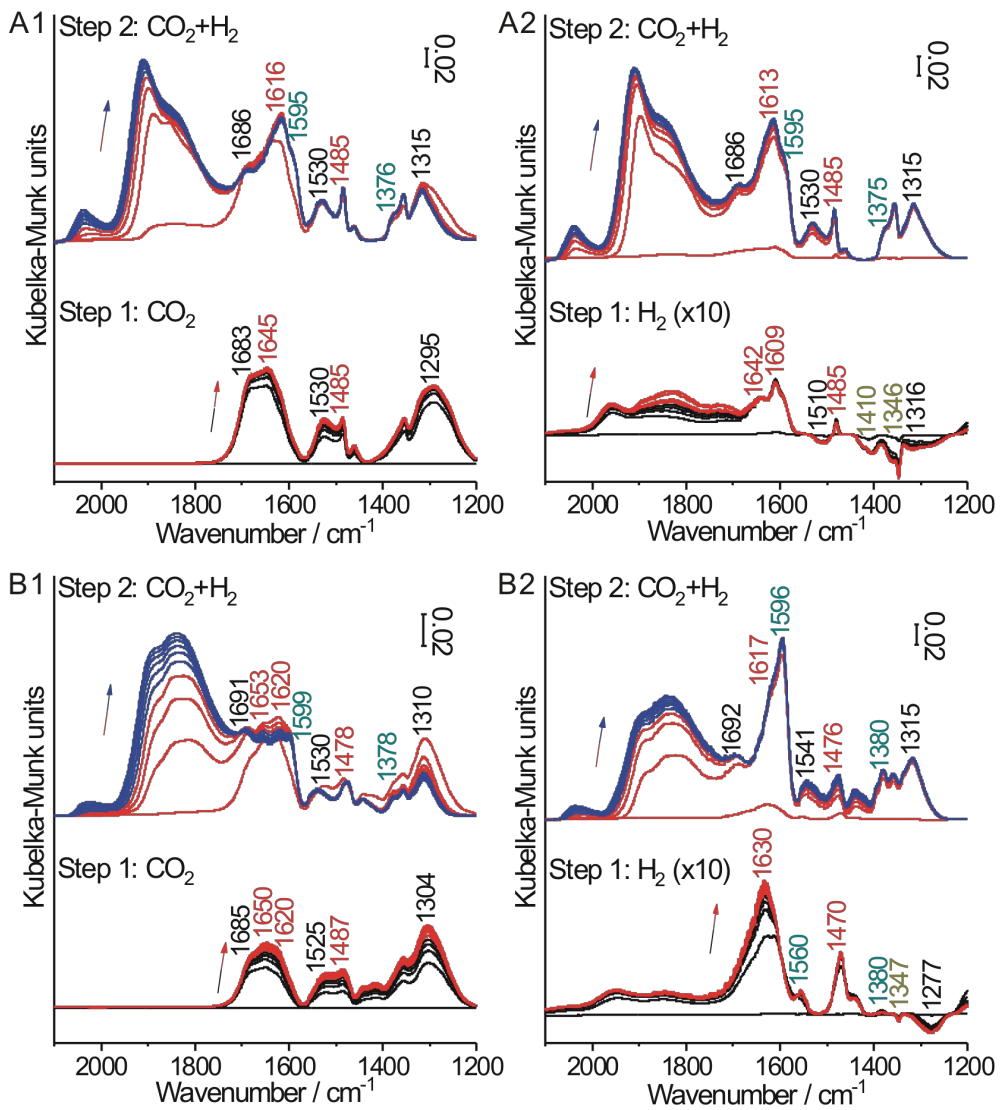


Figure S13. *In situ* time-resolved DRIFTS spectra of first CO_2 and then $\text{CO}_2 + \text{H}_2$ stepwise reactions at 373 K on (A1) 2%Pd/ZrO₂-M and (B1) 2%Pd/ZrO₂-T catalysts, and first H_2 and then $\text{CO}_2 + \text{H}_2$ stepwise reactions at 373 K on (A2) 2%Pd/ZrO₂-M and (B2) 2%Pd/ZrO₂-T catalysts. The colored arrow indicates the time progress and the time interval between two adjacent spectra is around three minutes with the total time for each gas treatment step of 30 minutes. Wavenumbers indicated at the plots are color-coded as follows: Black – bidentate carbonate, Red – bicarbonate, turquoise – formate and ochre – monodentate carbonate.

References

- (1) Wang, X.; Shi, H.; Kwak, J. H.; Szanyi, J. Mechanism of CO₂ hydrogenation on Pd/Al₂O₃ catalysts: kinetics and transient DRIFTS-MS studies. *ACS Catal.* **2015**, *5*, 6337-6349.
- (2) Köck, E.-M.; Kogler, M.; Bielz, T.; Klötzer, B.; Penner, S. In situ FT-IR spectroscopic study of CO₂ and CO adsorption on Y₂O₃, ZrO₂, and Yttria-Stabilized ZrO₂. *J. Phys. Chem. C* **2013**, *117*, 17666-17673.
- (3) Das, T.; Deo, G. Synthesis, characterization and in situ DRIFTS during the CO₂ hydrogenation reaction over supported cobalt catalysts. *J. Mol. Catal. A-Chem.* **2011**, *350*, 75-82.
- (4) Takano, H.; Kirihata, Y.; Izumiya, K.; Kumagai, N.; Habazaki, H.; Hashimoto, K. Highly active Ni/Y-doped ZrO₂ catalysts for CO₂ methanation. *Appl. Surf. Sci.* **2016**, *388*, 653-663.
- (5) Schild, C.; Wokaun, A. CO₂ hydrogenation over nickel/zirconia catalysts from amorphous precursors: on the mechanism of methane formation. *J. Phys. Chem.* **1991**, *95*, 6341-6346.
- (6) Weigel, J.; Koeppel, R. A.; Baiker, A.; Wokaun, A. Surface species in CO and CO₂ hydrogenation over copper/zirconia: on the methanol synthesis mechanism. *Langmuir* **1996**, *12*, 5319-5329.
- (7) Jeong, H.; Bae, J.; Han, J. W.; Lee, H. Promoting effects of hydrothermal treatment on the activity and durability of Pd/CeO₂ catalysts for CO oxidation. *ACS Catal.* **2017**, *7*, 7097-7105.